Biomass Conversion and Biorefinery
https://doi.org/10.1007/s13399-024-05283-0

ORIGINAL ARTICLE

Investigating the effect of process variables for ball milling of wood chips: energy demand and particle size

Carlos Arce[1] · Lukáš Krátký[1]

Received: 26 September 2023 / Revised: 27 November 2023 / Accepted: 3 January 2024

Abstract
Energy demand is the major drawback to using mechanical treatments within the biorefinery context. These treatments use energy to reduce particle size and crystallinity and, as a result, increase the accessibility of cellulose. However, the study of energy demand in milling needs to be more noticed. Therefore, this study aims to study how operational variables affect particle size and energy demand on one of the most used milling technologies: ball milling. The variables considered were mass of biomass, mass of balls and time. It was found that time is the most affecting variable for particle size and energy demand. Additionally, it was possible to optimise milling regarding energy demand and particle size. Furthermore, it was found that from the three traditional laws of comminution Bond was the one that gave the best results in terms of accuracy.

Keywords Beech chips · Biorefinery · Energy requirement · Ball mill · Particle size

1 Introduction

The world's population is continuously growing; thus, energy demand increases accordingly [1]. It is expected to increase to 8.5 billion by 2030 and reach nearly 10 billion by 2050 [2]. Nowadays, energy is obtained mainly from nonrenewable sources, either natural gas or fossil fuels. However, these natural resources are becoming scarce; therefore, alternative energy sources must be developed [3].

One alternative is lignocellulosic biomass (LCB) [4, 5]. It is the most significant renewable carbon source on the planet [6]. This biomass includes every plant and tree [2] and residues from agriculture, forestry, household and food industry, among others [7], thus contributing to the concept of circular economy. The composition of this biomass is mainly cellulose, hemicellulose and lignin, in different proportions [8], and the energy, through biofuels: biodiesel [9], bioethanol [10], biogas [11] and platform chemicals such as sorbitol, furfural [12]and levulinic acid [13], among. However, the nature of lignin and how it is interlinked with cellulose and hemicellulose and the crystalline-like behaviour of cellulose structure gives LCB a recalcitrant nature that hinders its processability [14]. Therefore, LCB needs to undergo pretreatment to avoid its structure's drawbacks.

Currently, a wide variety of pretreatments are available to increase the processability of LCB [15]. The classification is based on the driving force involved in the process. Physical treatments use energy to disrupt the matrix, thus reducing the crystallinity, resulting in an enhancement of sugar release. Depending on how the energy is applied, physical pretreatments can be classified as mechanical [16], microwaves [17] and ultrasonication [18]. Chemical pretreatments use chemicals that can cleavage the bonds between the components of the LCB structure. Alkaline treatment [19], acid hydrolysis [20] and novel solvents such as Ionic liquids or deep eutectic systems [21, 22] are the techniques available. Biological pretreatments use microorganisms such as bacteria and fungi [23, 24]. These pretreatments promote the degradation of lignin and cellulose by the action of the enzymes they produce. Finally, the combination of physical and chemical pretreatments can be classified separately as physicochemical. It takes advantage of the physical changes the chemicals involved go through when the reaction conditions change drastically, i.e., steam explosion and CO_2 explosion, among others [25, 26].

Among the available pretreatments described previously, physical treatment is the one that is always used when processing LCB, more specifically, mechanical treatment. As

✉ Carlos Arce
Carlos.Arce.Gutierrez@cvut.cz

[1] Faculty of Mechanical Engineering, Czech Technical University in Prague, Technická 4Dejvice, Prague 6 160 00, Czech Republic

mentioned, these pretreatments use energy to disrupt the cell wall and make cellulose more accessible by reducing crystallinity and increasing specific surface area. Additionally, the size is reduced, which increases manageability and bulk density. The technology available for mechanical size reduction is very well documented; knife mill [27], hammer mill [28], centrifugal mill [16], rod mill [29] and ball mill [30] are the most common. The ball mill is the most used in the literature [1]. Even though this technology has advantages, energy demand and scale-up are its most significant drawbacks. However, only some studies have focused on researching and optimising energy demand and particle size. Therefore, this article aims to analyse the effect of process parameters for ball-milled wood chips on energy demand and particle size.

2 Materials and methods

2.1 Biomass pretreatment

Biomass in this study was beech wood chips. These chips were left open to the air to reach ambient moisture content. Moisture was measured by drying the sample at 105 °C in a dryer KBC-25W (Binder Ltd., Tuttlingen, Germany) to constant weight, reaching a value of 7.77 ± 0.01% wt. Initially, the piece was mechanically pretreated to homogenise it. The pretreatment was performed in an SM300 knife mill (Retsch Ltd. Haan, Germany) at 3000 rpm and a 10 mm sieve. Particle size distribution was evaluated using a shaker and the following sieving sizes: 10 mm, 7 mm, 5 mm, 2.5 mm, 0.9 mm, 0.85 mm, 0.71 mm, 0.6 mm, 0.45 mm, 0.28 mm and 0.15 mm. Each sieve was weighed after and before to obtain the mass fraction using an analytical balance PCB 6000–1 (Kern & Sohn, Ballingen, Germany).

2.2 Particle size distribution

These analyses were performed according to the standard "method of determining and expressing particle size of chopped forage material by screening" [31]. The Rosin–Rammler-Sperling-Bennet (RRSB) distribution was used since it is the one recommended by the ASABE standard and is described by Eq. 1.

$$F = 1 - e^{-\left(\frac{D}{D_P}\right)^n} \tag{1}$$

where F (-) is the accumulated mass fraction smaller than D (mm), D_P (mm) represents a characteristic parameter of the distribution that corresponds to the diameter at the fraction equal to 63.2%, and n (-) is a parameter that indicates the dispersity of the distribution. The characteristic parameters can be calculated from the experimental data using the linearisation of the previous equation leading to Eq. 2.

$$\ln(-\ln(1 - F)) = n \cdot \ln(D) - n \cdot \ln(D_p) \tag{2}$$

where n is the slope of the data extracted from the sieve analysis and $n{\cdot}\ln D$ is the intercept with the y-axis. The parameters of the RRSB distribution, D_P and n, were reached by linear regression with the least square method. Knowing RRSB parameters, the values of D_F can be determined according to Eq. 3.

$$D_F = D_P(-ln(1 - F))^{1/n} \tag{3}$$

Finally, D_{10}, D_{50} and D_{90} particle size parameters were calculated by Eq. 3 for individual experimental runs, changing the F value accordingly. As the most representative value, particle size D_{50} was used for further modelling steps.

2.3 Milling experiments

Size reduction of biomass was carried out using a Drum Mill TM 300 (Retsch Ltd., Haan, Germany). The attrition material inside the mill was stainless steel balls of 3 mm diameter. The rotating critical speed of the mill (Nc) was calculated using Eq. 4 [32]. The size reduction principle in ball mill is based on both breaking and tearing. On the one side, the milling drum rotates and the milling elements too, thus, falling and breaking the biomass. On the other side, biomass is comminuted by the tear forces between the milling elements (balls) and between those and the shell as well. To reach the dominance of breaking and avoid the centrifugal effect of the batch, the recommended drum rotational speed must be equal to

$$Nc = \frac{42.3}{\sqrt{D_m - d_B}}$$

where D_m is the diameter of the mill drum (30 cm) and d_B is the diameter of the attrition material (3 cm). With these values, Nc equals 81.41 rpm, similar to the maximum value that can be used for the mill. Therefore, it was decided to operate the mill at a percentage of the maximum critical speed, for safety. The value of the speed was 75% of the maximum value for the mill, since it is lower than the critical speed, for safety reasons and to operate the mill properly.

Initially, the required mass of beech chips and attrition material is loaded in the mill, and the time starts, depending on the experiment. Energy demand was measured using a Fluke 438 Series II Power Analyzer (Fluke Corporation, Everett, WA, US) with a time step of 1 s. The idle power of the machine was also recorded by running the mill without sample or attrition material. Energy demand was calculated by Eq. 4.

$$e_c = \int_0^t P_T dt - \int_0^t P_{\mathrm{IDLE}} dt \quad (4)$$

where e_c (Ws) is the comminution energy, P_T (W) is the power measured when biomass was introduced in the mill, t(h) is the milling time and P_{IDLE} (W) is the power measured without biomass in the mill. P_T and P_{IDLE} were calculated using the trapezoidal rule. Specific energy demand e (Ws g^{-1}) was calculated using Eq. 5.

$$e = \frac{e_c}{m} \quad (5)$$

where m (kg) and e_c (Ws) are the comminution energy obtained in Eq. 4 and are the mass of biomass processed in the run (Eq. 5).

2.4 Experimental design

The design of experiments was carried out using Statgraphics Centurion 19. It was carried out following a three-level-three-factor Box-Benhken, with three central points, based on response surface methodology. This method has been widely used in industry and research to analyse the effects on the process and optimise [33–35]. Additionally, it allows to obtain results with the least experiments possible. In this work, time (h), mass of balls (kg) and mass of biomass (kg) were the effects. The objective was to minimise energy demand (kWh·t^{-1}) and D_{50} (mm). For the fitting of the experimental data, a second-order polynomial was used (Eq. 6). Table 1 shows the codification of the experiments and the range of values.

$$Y = b_0 + \sum b_i \cdot X_i + \sum b_{ii} \cdot X_i^2 + \sum b_{ij} \cdot X_i \cdot X_j \quad (6)$$

In Eq. 6, Y is the dependent variable considered, either energy or D_{50}, $X_{i,j}$ is the factors (biomass, balls and time) and b_{ij} is the coefficients obtained by Statgraphics.

Table 1 Factors and levels for the experimental design

Run	Biomass (kg)	Balls (kg)	Time (h)
1	1	0	1
2	1	−1	0
3	−1	0	0
4	0	1	−1
5	0	−1	−1
6	1	0	−1
7	−1	0	−1
8	1	1	0
9	−1	0	1
10	0	1	1
11	−1	1	0
12	0	−1	1
13	0	0	0
14	0	0	0
15	0	0	0
Factors	Levels		
Biomass (kg)	0.1	0.3	0.5
Balls (kg)	5	12.5	20
Time (h)	1	4.5	8

3 Results

Particle size distribution was evaluated using the RRSB distribution. The application of this distribution was confirmed by the influence of time on particle size. This set of experiments was performed aside from the ones obtained by the experimental design; the application of the RRSB distribution needed to be verified before any investigation was conducted. Figure 1 shows the RRSB distribution vs. the observed values.

Time has a significant effect on particle size, as was expected. This influence is especially significant in the first 4 h of milling. However, from 6 to 8 h, the difference in particle size is negligible since the curves are close to each other; this influence allowed the authors of this research to choose a suitable maximum milling time. As can be seen from the previous graph, modelled results fitted the observed results. Therefore, this distribution will be used to obtain the values for particle sizes D_{10}, D_{50} and D_{90}. Table 2 shows the parameters of the RRSB distribution for the experiments from the factorial design.

Regarding the accuracy of the distribution, in terms of R^2 values, all the experiments had values above 0.8, and most deals were above 0.9. This distribution has been used for several grinding processes and has been proven to describe particle size appropriately [36, 37]. From Table 2, time is the most affecting energy and particle size variable. This can be seen when comparing experiments 6 and 1, 4 and 10 and 5 and 12, where D_{50} was reduced from 0.932 to 0.039 mm, from 0.543 to $5 \cdot 10^{-3}$ mm and from 1.21 to 0.105, respectively. Additionally, the mass of wood influences particle size, but unlike time, increasing biomass has a dampening effect on particle size, as seen in experiments 2 and 3. Experiment 2 has a final particle size of 0.9 mm after 4.5 h using 0.5 kg of biomass. However, experiment 3, performed simultaneously using 0.1 kg of biomass, reaches a D_{50} of 0.064 mm. This is the result of the dampening effect of the biomass. Already milled biomass gets stacked on the balls, thus reducing the impact of the forces that generate the size reduction. The problems that the agglomeration of particles produced on reducing the efficiency of ball milling have been previously reported. It prevents particle size from being reduced further than a specified limit. Other authors

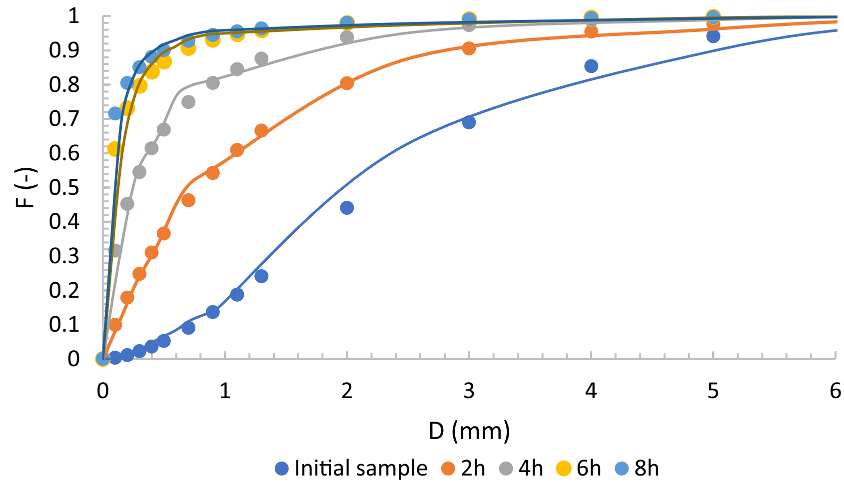

Fig. 1 RRSB distribution function for ball-milled biomass at different times: 69 rpm, 0.3 kg biomass and 8 kg balls. Lines are simulated values and dots are experimental values

Table 2 Parameters of the RRSB distribution for each experiment

Experiment	Biomass (kg)	Balls (kg)	Time (h)	Energy (kWh·t^{-1})	D_p (mm)	D_{50} (mm)	n	R^2
0	Pretreatment				3.253	2.63	1.733	0.994
1	0.5	12.5	8	889.52	0.096	0.039	0.414	0.806
2	0.5	5	4.5	189.38	1.375	0.900	0.865	0.997
3	0.1	5	4.5	396.04	0.141	0.064	0.468	0.979
4	0.3	20	1	294.20	0.950	0.543	0.655	0.992
5	0.3	5	1	116.50	1.750	1.213	1.001	0.995
6	0.5	12.5	1	124.57	1.396	0.932	0.907	0.994
7	0.1	12.5	1	565.19	0.630	0.343	0.603	0.981
8	0.5	20	4.5	654.92	0.171	0.073	0.433	0.923
9	0.1	12.5	8	4112.35	0.004	1.00E-03	0.210	0.900
10	0.3	20	8	1258.36	0.018	5.00*E*-03	0.295	0.865
11	0.1	20	4.5	1043.46	0.040	1.00*E*-02	0.257	0.844
12	0.3	5	8	601.33	0.212	0.105	0.520	0.956
13	0.3	12.5	4.5	746.36	0.226	0.095	0.422	0.985
14	0.3	12.5	4.5	793.32	0.273	0.114	0.420	0.979
15	0.3	12.5	4.5	711.86	0.234	0.099	0.428	0.974

found that increasing the energy of the milling process did not improve particle size reduction and reached a plateau at around 300 nm for silica particles [38]. This effect was also found in the size reduction of inkjet application ink [39]. The same result was found for ball-milled wheat straw. D_{50} reduced from around 100 to about 20 µm, and increasing energy would not reduce particle size further [40]. In the current study, the same effect is reported, especially at high loads of biomass and high times, showing no significant reduction in the highest energy demand. Energy demand has a similar trend when compared to particle size. Time has the most significant influence, as expected since energy demand for the longest time is the highest. Additionally, the quantity of biomass has an exciting effect on energy demand since increasing biomass reduces energy demand. It can be explained by the reduced matter deposits in the bottom of the milling chamber, ameliorating the rebound generated by the falling balls. Experiments 1 and 9 show this effect. While experiment 1 has an energy demand of 889.52 kWh·t^{-1}, experiment 9 shows an energy demand of 4112.35 kWh·t^{-1}, showing a fourfold decrease while increasing four times the mass of biomass. Other authors found similar values for comminution energy. Some authors found energy values of 500 kWh·t^{-1} and 2150 kWh·t^{-1} for reduction ratios of 66% and 87%, respectively, for the comminution of Douglas fir to increase sugar yield [41]. However, other researchers found higher values for energy demand for similar reduction ratio values. For a reduction ratio of 74%, energy demand was 3020 kWh·t^{-1} [40]. In the current study, the values are lower than the previously cited research; however, values are very similar if total energy is considered. For a 65% reduction ratio, energy demand was 189.38 kWh·t^{-1} (1576 kWh·t^{-1}

Table 3 Coefficients and p-values for the mathematical model of D_{50} and energy demand

Ball milling factor	Y_1: D_{50}		Y_2: energy	
	b_{ij}	p-values	b_{ij}	p-values
Intersection	0.972455	-	− 1105.09	-
X_1: biomass	3.2897	0.0011	− 2879.42	0.0731
X_2: balls	− 0.0792582	0.0008	250.985	0.3482
X_3: time	− 0.26998	0.0001	201.012	0.0281
X_1X_1	0.266667	0.8083	8446.82	0.3741
X_1X_2	− 0.128833	0.0048	− 30.3134	0.8966
X_1X_3	− 0.196786	0.0185	− 993.646	0.0909
X_2X_2	0.00263852	0.0162	− 9.19889	0.1954
X_2X_3	0.00542857	0.0163	4.56505	0.7335
X_3X_3	0.017585	0.0036	27.308	0.3785

total energy), and for an 86% reduction ratio, energy demand was 565.19 kWh·t^{-1} (2094.57 kWh·t^{-1} total energy).

3.1 Mathematical model and statistical analysis: effect of process variables on D_{50} and energy demand

The process variables' effect and mathematical model were analysed in-depth using Statgraphics Centurion 19 software. It allows the design of experiments to be carried out, so data can be analysed to find effects and relationships between the dependent and the independent variables. Table 3 shows the coefficients of the model.

Using the coefficients from the previous table and Eq. 6, a mathematical expression can be used to predict the values of D_{50} and energy demand using only the process parameters. Additionally, it was possible to build the Pareto plots using the p-values from the table. The p-value can help to decide if a factor significantly affects the dependent variable. If the p-value is lower than 0.05, this factor has a significant effect with a 95% confidence level. Figure 2 shows the Pareto plots.

As can be seen from the parity plots regarding D_{50}, all the factors have a significant effect on reducing particle size, except for the term A^2. Therefore, when using the mathematical expression for D_{50}, the only factor that can be erased without affecting accuracy significantly is A^2. On the other hand, regarding energy, time is the only factor that affects energy demand significantly. Therefore, there is a linear dependence between energy and time. After the effects of the elements were obtained, a statistical analysis of the model was also carried out through the ANOVA table. It helped to indicate the robustness and significance of the model. Table 4 shows the statistical values (ANOVA analysis) for both models.

From the statistical analysis shown in Table 3, the p-value of the model for D_{50} is lower than 0.05. This means that the model is statistically significant, with a 95% confidence level. Therefore, the factors considered in the design of experiments can be used to predict D_{50}. Furthermore, regarding accuracy, this expression fits the experimental data well since the R^2 value is 98.57% and the adjusted value is 96%. On the other hand, the mathematical expression for energy meets different requirements. The p-value for the model is higher than 0.05, which means that the factors considered cannot predict energy changes. From an accuracy point of view, the R^2 value; however, the adjusted R^2 value is lower; therefore, the mathematical expression for energy is not statistically significant, and its accuracy needs to be better.

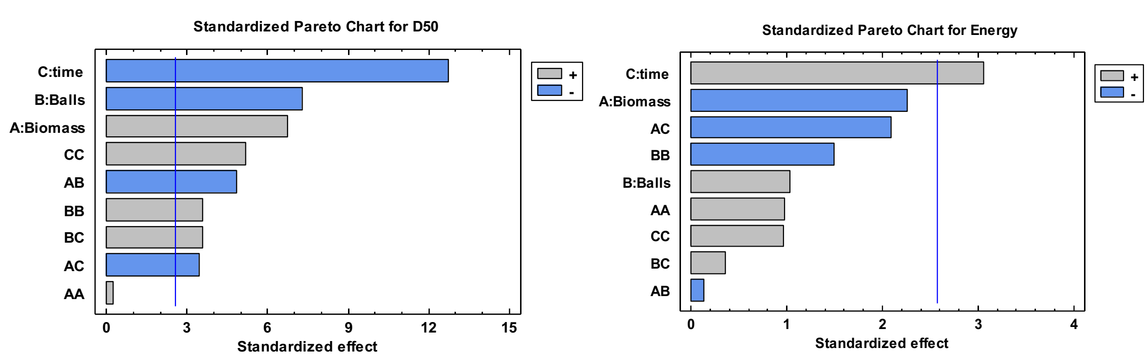

Fig. 2 Pareto plots for D_{50} and energy demand

Table 4 ANOVA table for both models

	Transformation	Model d.f	p-value	Error d.f	Stnd. error	R^2	Adj. R^2
Energy	None	9	0.1411	5	666	83.06	52.57
D_{50}	None	9	0.0004	5	0.0801	98.57	96

Therefore, the mathematical expression could not predict the results regarding energy. As a result, it was decided to change the data pool from energy. The hypothesis behind these results is that the gap between energy demand values is huge. For example, experiment 9 has an energy demand of more than 4000 kWh·t^{-1} and experiment 5 is just above 100 kWh·t^{-1}, which is about 40 times higher. So, to reduce this gap, it was decided to use the logarithm of the values of energy instead of the raw values. Figure 3 shows the new values for the factors and the statistical analysis of the model, with the logarithm transformation in energy and the new Pareto chart.

The transformation of the energy raw values into the logarithm values lead to an increase in the accuracy of the mathematical model from 83 to 95.34%. The factors that significantly influence energy demand also increased; the mass of biomass, the mass of balls and the squared effect of balls were added as significant since the *p*-values for these effects were lower than 0.05. From the previous Pareto plots, time increases energy demand, which makes sense since the more time the mill works, the higher the energy demand. The same effect occurs with the mass of balls. On the other hand, the mass of biomass reduces energy demand. This effect was confirmed in Table 1. Increasing the mass of biomass reduces energy demand because it dampens the impact of falling balls. Furthermore, the statistical analysis also improved since the *p*-value of the model became lower than 0.05, which, unlike the raw values, makes it statistically significant with a 95% confidence level. Therefore, this model will be the one used forward.

Finally, when the mathematical expressions for D_{50} and energy demand were obtained, it was possible to obtain the surface response surfaces to find the optimum values for both independent variables to minimise energy and particle size (Fig. 4).

Regarding energy, time is the operational parameter with the highest influence since the slope from Fig. 4a, c in the time axis is the most significant. This effect is also confirmed in Fig. 1. On the other hand, biomass has the opposite effect since increasing biomass reduces energy demand. Therefore, fast times and high biomass load are recommended to obtain the lowest energy demand possible. The mass of balls increases energy demand for low values, from 5 to 14 kg. However, from 14 to 20 kg, the effect is negligible. As a result, the optimisation values to minimise energy demand should be in the region of short times (2–4 h), low mass of balls (5–11 kg) and high biomass load (0.3–0.5 kg). From the point of view of particle size (Fig. 4b, d, f), time also

Ball milling factor	Y_2: Energy	
	b_{ij}	p-values
Intersection	4.05924	-
X_1: Biomass	-4.08433	0.0064
X_2: Balls	0.28762	0.0093
X_3: time	0.357342	0.0007
X_1X_1	1.48938	0.7457
X_1X_2	0.0453283	0.7007
X_1X_3	-0.00671088	0.9786
X_2X_2	-0.00914364	0.0315
X_2X_3	-0.00179	0.7897
X_3X_3	-0.00903871	0.5521
Statistical analysis		
Model	Energy	
Model d.f.	9	
P-value	0.0078	
Error d.f.	5	
Standard error	0.334	
R^2	95.34	
Adjusted R^2	86.94	

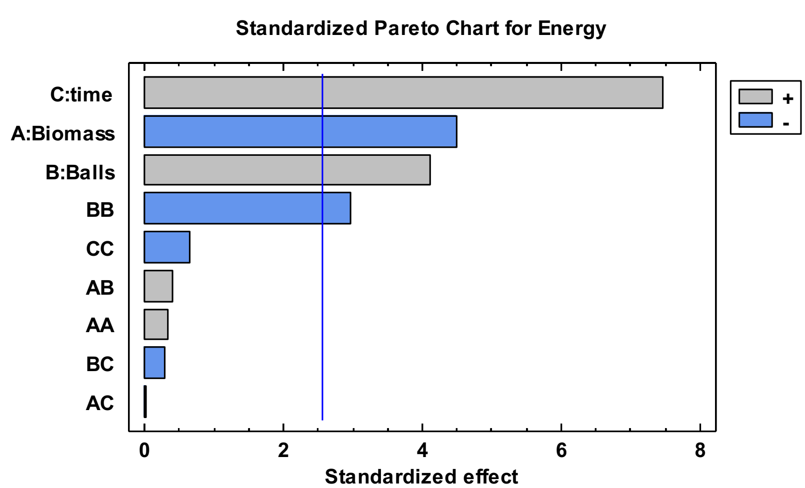

Fig. 3 Statistical analysis and Pareto chart for the logarithm transformation of energy

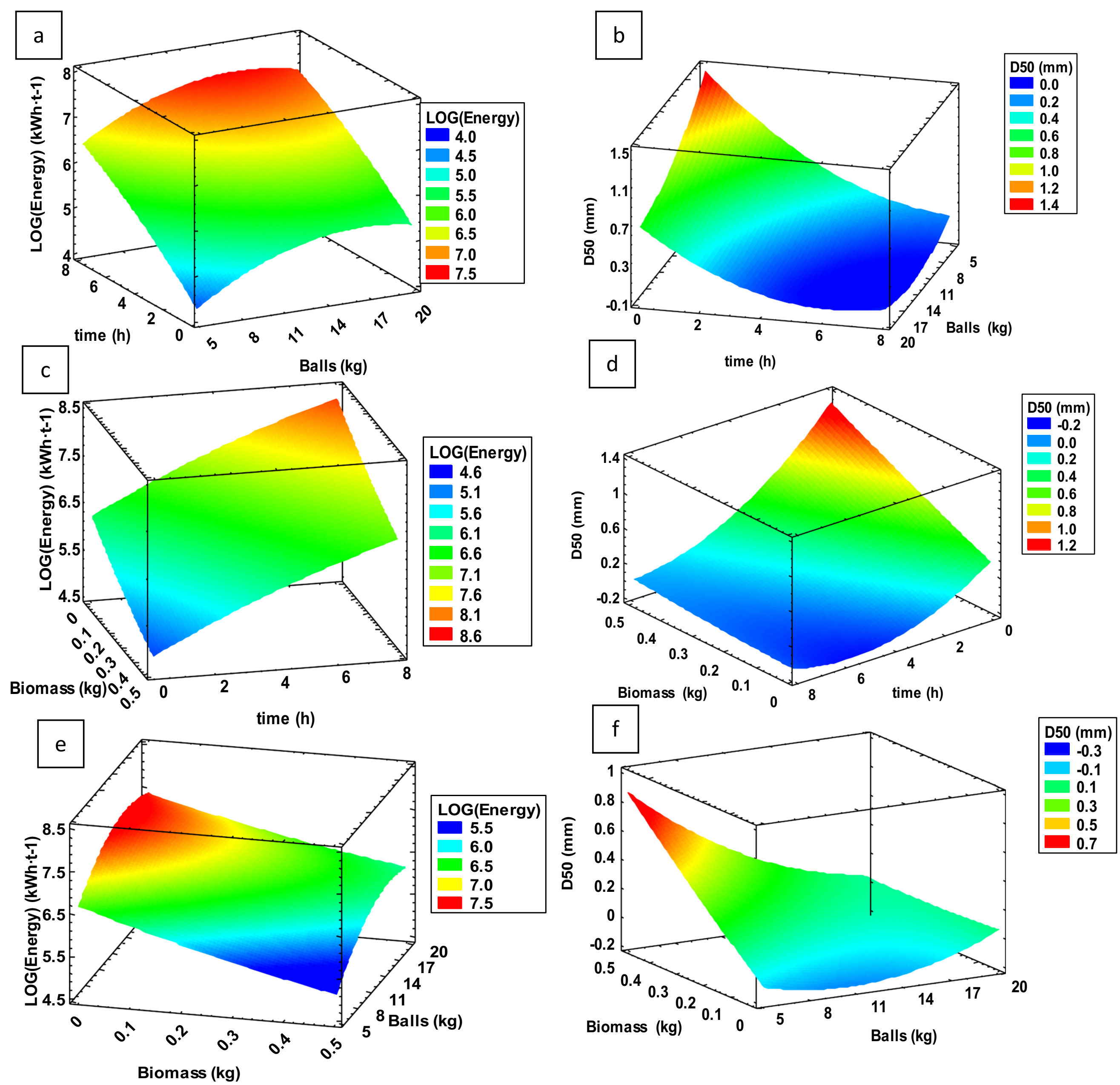

Fig. 4 Response surfaces for energy (**a**, **c**, **e**) and D_{50} (**b**, **d**, **f**)

has the most significant effect. It decreases from the beginning. However, there is a point where particle size is not reduced further; from 4 h, the effect of time starts to fall, and up to 6 h milling time, particle size is not reduced more. Therefore, the time of milling should be at most 4 h. It was found that increasing biomass load has an interesting effect on D_{50}, especially at short times and low mass of balls. However, increasing milling time and the quantity of balls lead to smaller sizes. The powder generated by the mill agglomerated on the surface of the balls, thus reducing the effectivity of the grinding process. For times longer than 4 h, the mass of balls has nearly no effect on particle size because it reached a minimum at this milling time. The effect of balls is more significant for shorter times (<4 h). In this region, as seen in Fig. 4b, D50 is the smallest at increasing mass of balls. The green region can show this. In the graphs, some areas are below zero; these regions should not be considered a good result because size cannot be negative. So, these regions will not be considered in the optimisation.

The trends shown in Fig. 3b, d, f are similar to those found by [42]; in this study, B_4C powder was used. However, the effect of the milling conditions is similar. The most

Table 5 Optimization results for energy and D_{50}

Energy ($kWh \cdot t^{-1}$)	D_{50} (mm)	Biomass (kg)	Balls (kg)	Time (h)
345	0.295	0.472	19	2.74

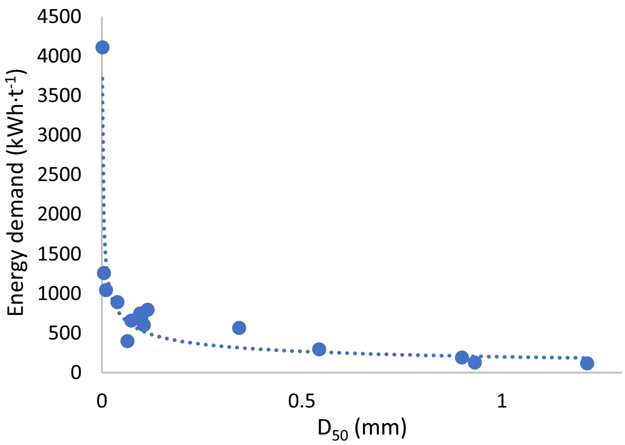

Fig. 5 Relationship between energy and D_{50}

affecting variable considered was time. It should be noted that the mass of balls and biomass were joined in a ratio.

Finally, the optimisation shown in Table 5 was carried out with the considerations highlighted before. The conditions were to minimise particle size and energy demand, and the equations to calculate them were developed by the software with the coefficients from Table 2, for particle size and Fig. 3, for energy. The minimum limits for size and energy were 0.3 mm and 350 $kWh \cdot t^{-1}$, respectively. The limits for the independent variables were set by those chosen on the experimental factorial design.

3.2 Comparison of the results with the traditional comminution laws

Obtaining the optimum conditions to minimise energy and size and, as a result, the costs of the process is a valuable tool. However, it would only be complete with the relationship between particle size and energy demand. Figure 5 shows the relationship between energy and D_{50}.

The relationship shown in the previous figure has been extensively studied. Researchers have found the same trend for the milling of amaranth grain [43], Douglas fir [41] or wheat straw [40] using a planetary ball mill.

Traditionally, this relationship has been calculated by the traditional comminution laws, being Kick, Bond and Rittinger, using the generic expression that follows (Eq. 6).

$$E = \frac{C}{r-1} \cdot \left[\frac{1}{D^{r-1}} - \frac{1}{D_0^{r-1}} \right] \tag{7}$$

where E is the energy demand, C is a constant, r is a model parameter which depends on the law used and is non-dimensional, D is the final particle size, and D_0 is the initial particle size; in this work, it was 2.63 mm. According to the literature, the energy used in Eq. 6 is exclusively needed for the comminution of the particle. Measuring this energy is challenging, especially in ball milling, since most of the energy is lost in the collision between balls [44]. That is the reason why energy demand values used are the difference between total energy and idle energy. Although these laws were initially developed for the mining industry, several authors have applied them to the comminution of biomass [45, 46]. Therefore, they were applied in this work, and a parametric analysis using the generic expression (Eq. 6) was carried out to find the values of C and r. Table 6 shows the comminution laws' values and the parametric analysis.

The three comminution laws give accuracy results, in terms of the regression coefficient, higher than 70%. However, the parametric model gave an accuracy of 90.98% regarding the R^2 value. The comminution constant was 94.2 $kWh \cdot t^{-1} \cdot mm^{0.4}$, and the r value was 1.42. Regarding the three comminution laws, the most accurate with the set of data was Bond's law which agrees with the bibliography since Bond's law is said to describe ball milling behaviour the best[47].

3.3 Validation

The validation of the model was performed by carrying out additional experiments at different conditions used for the development of the model but within the maximum and minimum values of the independent variables. The results

Table 6 Results for the traditional laws of comminution and the parametric model of the general expression

	Bond	Rittinger	Kick	Parametric model
Constant	53.6 ± 5.889^a	17.29 ± 2.89	1209.81 ± 160.6	94.2 ± 22.6
r	1.5	2	1	1.42 ± 0.056
R^2	85.55	71.92	80.2	90.98
Mean absolute error	1545.82	2328.61	1768.4	237.096

[a]work index

Table 7 Results and conditions used for the validation

Experiment	Biomass	Balls	Time	Experimental energy	Energy simulated	Experimental D_{50}	Simulated D_{50}
16	0.3	12.5	4.5	7.52	6.91	0.0248	0.0044
17	0.3	12.5	4.5	6.39	5.99	0.330	0.369
18	0.3	12.5	4.5	6.18	6.38	0.346	0.328

will be compared to those obtained with the model to assess whether it can replicate the experimental values with good accuracy. Table 7 shows the results and the conditions of the experiments.

As can be seen, the model developed can replicate the results obtained experimentally, especially for experiments 17 and 18. Regarding energy, it can be said that the model can predict the energy demand just with the conditions.

Regarding experiment 16, the difference between the experimental and the modelled is higher than expected. However, it should be noted that the values for D_{50} under these conditions are very small; therefore, measurements other than screen sieve analysis should be performed. On the other hand, D_{50} values below 0.3 mm are not commonly used within the biorefinery concept, in fact, according to the bibliography, the recommended particle size for the successful hydrolysis of biomass is between 1 and 2 mm [48], and in this range of values, the model is accurately enough. For the assessment of the accuracy of the model, the parity plots were obtained (Fig. 6).

As can be seen from the previous figure, the model predicts accurately the energy values and is always below 10% error. Regarding D_{50} there is some when simulated values are compared to experimental ones, especially a size below 0.2 mm. However, as it was stated before, these values are not frequently used for biomass valorisation under the biorefinery concept.

4 Conclusions

In this work, the effect of process parameters (milling time, mass of biomass and mass of balls) on ball milling of wood chips has been assessed. Regarding D_{50}, it was found that all the factors considered affected particle size except for the quadratic term for biomass. The energy was more affected by time; however, accuracy was low ($R^2 = 83.06$). Therefore, it was decided to transform the results for energy to the logarithmic values. With this transformation, R^2 was increased to 95.34, and it was found that time biomass and balls, as well as the quadratic term of mass of balls, were the most affecting factors.

Additionally, it was possible to obtain a relationship between energy demand and particle size. The traditional comminution law that is more suitable for ball milling was Bond, which agrees with the literature found. However, a parametric model showed that the most suitable values for the constant and r values in the generic expression of the comminution laws were 94.2 and 1.42, respectively.

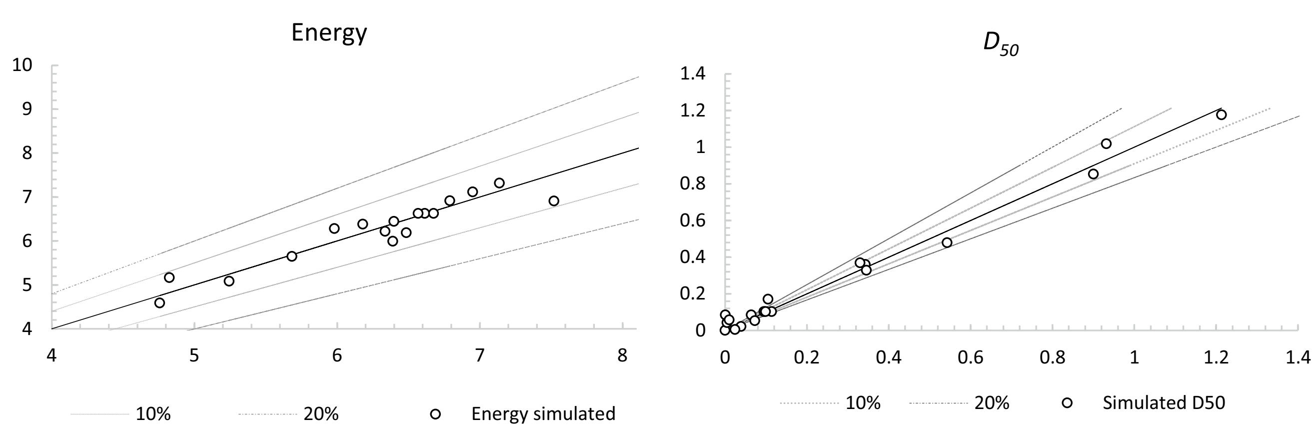

Fig. 6 Parity plots for D_{50} and energy for ball milling

Acknowledgements The authors would like to acknowledge the CTU Global Postdoc Fellowship Program.

Author contribution Conceptualization: LK. Methodology: CA and LK. Investigation: CA. Validation: CA and LK. Formal analysis: CA. Writing the draft: CA. Review: LK. Supervision: LK. Project administration: LK. All authors have read and agreed to the published version of the manuscript.

Funding Open access publishing supported by the National Technical Library in Prague. This research was supported by the Ministry of Education, Youth and Sports of the Czech Republic under OP RDE grant number CZ.02.1.01/0.0/0.0/16_019/0000753 "Research centre for low-carbon energy technologies".

Data availability The data that support the findings of this study are available from the corresponding author upon reasonable request.

Declarations

Ethics approval Not applicable.

Competing interests The authors declare no competing interests.

References

1. Arce C, Kratky L (2022) Mechanical pretreatment of lignocellulosic biomass toward enzymatic/fermentative valorization. iScience 25:104610. https://doi.org/10.1016/j.isci.2022.104610
2. Llano T, Arce C, Gallart LE et al (2023) Techno-economic analysis of macroalgae biorefineries: a comparison between ethanol and butanol facilities. Fermentation 9:1–16. https://doi.org/10.3390/fermentation9040340
3. Arhin SG, Cesaro A, Di Capua F, Esposito G (2023) Recent progress and challenges in biotechnological valorization of lignocellulosic materials: towards sustainable biofuels and platform chemicals synthesis. Sci Total Environ 857:159333. https://doi.org/10.1016/j.scitotenv.2022.159333
4. Velvizhi G, Goswami C, Shetti NP et al (2022) Valorisation of lignocellulosic biomass to value-added products: paving the pathway towards low-carbon footprint. Fuel 313:122678. https://doi.org/10.1016/j.fuel.2021.122678
5. Tey TO, Chen S, Cheong ZX et al (2021) Synthesis of a sustainable integrated biorefinery to produce value-added chemicals from palm-based biomass via mathematical optimisation. Sustain Prod Consum 26:288–315. https://doi.org/10.1016/j.spc.2020.10.012
6. Yang G, An X, Yang S (2021) The effect of ball milling time on the isolation of lignin in the cell wall of different biomass. Front Bioeng Biotechnol 9:. https://doi.org/10.3389/fbioe.2021.807625
7. Zhou C, Wang Y (2020) Recent progress in the conversion of biomass wastes into functional materials for value-added applications. Sci Technol Adv Mater 21:787–804. https://doi.org/10.1080/14686996.2020.1848213
8. Ge X, Chang C, Zhang L et al (2018) Conversion of lignocellulosic biomass into platform chemicals for biobased polyurethane application, 1st ed. Elsevier Inc:. https://doi.org/10.1016/bs.aibe.2018.03.002
9. Jan HA, Osman AI, Al-Fatesh AS et al (2023) Biodiesel production from Sisymbrium irio as a potential novel biomass waste feedstock using homemade titania catalyst. Sci Rep 13:11282. https://doi.org/10.1038/s41598-023-38408-y
10. Hamadou B, Djomdi D, Zieba Falama R et al (2023) Optimization of energy recovery efficiency from sweet sorghum stems by ethanol and methane fermentation processes coupling. Bioengineered 14:228–244. https://doi.org/10.1080/21655979.2023.2234135
11. Jin Y, Hu J, Su J et al (2023) Improved bioenergy value of residual rice straw by increased lipid levels from upregulation of fatty acid biosynthesis. Biotechnol Biofuels Bioprod 16:1–14. https://doi.org/10.1186/s13068-023-02342-y
12. Zhang Z, Tao F, Ji H (2023) Valorization of Boehmeria nivea stalk towards multipurpose fractionation: furfural, pulp, and phenolic monomers. Biotechnol Biofuels Bioprod 16:1–11. https://doi.org/10.1186/s13068-023-02351-x
13. Helmi MRA, Rahayu DUC, Pratama AP et al (2023) Comparative study of microwave-assisted versus conventional heated reactions of biomass conversion into levulinic acid over hierarchical Mn3O4/ZSM-5 zeolite catalysts. Carbon Resour Convers 6:245–252. https://doi.org/10.1016/j.crcon.2023.02.005
14. Pang J, Zheng M, Li X et al (2019) Unlock the compact structure of lignocellulosic biomass by mild ball milling for ethylene glycol production. ACS Sustain Chem Eng 7:679–687. https://doi.org/10.1021/acssuschemeng.8b04262
15. Shukla A, Kumar D, Girdhar M et al (2023) Strategies of pretreatment of feedstocks for optimized bioethanol production: distinct and integrated approaches. Biotechnol Biofuels Bioprod 16:1–33. https://doi.org/10.1186/s13068-023-02295-2
16. Areepak C, Jiradechakorn T, Chuetor S et al (2022) Improvement of lignocellulosic pretreatment efficiency by combined chemo - mechanical pretreatment for energy consumption reduction and biofuel production. Renew Energy 182:1094–1102. https://doi.org/10.1016/j.renene.2021.11.002
17. Yadav N, Yadav G, Ahmaruzzaman M (2023) Microwave-assisted biodiesel production using –SO3H functionalized heterogeneous catalyst derived from a lignin-rich biomass. Sci Rep 13:1–17. https://doi.org/10.1038/s41598-023-36380-1
18. Shetty K, Krishnakumar G (2023) Strategies to enhance lipid productivity in microalgae: role of cell disruption and media composition. Fuel 345:128240. https://doi.org/10.1016/j.fuel.2023.128240
19. Dou X, Tang Y (2017) The influence of cold caustic extraction on the purity, accessibility and reactivity of dissolving-grade pulp. ChemistrySelect 2:11462–11468. https://doi.org/10.1002/slct.201701551
20. Hancock J, Osei-Bonsu R, Hoque M et al (2023) Valorization of cannabis green waste to cellulose nanomaterials via phosphoric acid hydrolysis. Ind Crops Prod 201:116888. https://doi.org/10.1016/j.indcrop.2023.116888
21. Liang X, Huang Z, Zhang J, Guo Y (2023) Ionic liquid recovery and recycling via electrodialysis in biomass processing: an economical assessment. Bioresour Technol 384:129332. https://doi.org/10.1016/j.biortech.2023.129332
22. Ling Z, Tan Y, Li X et al (2023) Elucidating multi-scale deconstruction of bamboo crystalline cellulose by novel acetylcholine chloride based deep eutectic solvents for enhanced enzymatic

hydrolysis. Ind Crops Prod 203:117156. https://doi.org/10.1016/j.indcrop.2023.117156
23. Mustafa AM, Poulsen TG, Sheng K (2016) Fungal pretreatment of rice straw with Pleurotus ostreatus and Trichoderma reesei to enhance methane production under solid-state anaerobic digestion. Appl Energy 180:661–671. https://doi.org/10.1016/j.apenergy.2016.07.135
24. Zhang D, Luo Y, Chu S et al (2015) Biological pretreatment of rice straw with streptomyces griseorubens JSD-1 and its optimized production of cellulase and xylanase for improved enzymatic saccharification efficiency. Prep Biochem Biotechnol 46:575–585. https://doi.org/10.1080/10826068.2015.1084932
25. Zhang W, Diao C, Wang L (2023) Degradation of lignin in different lignocellulosic biomass by steam explosion combined with microbial consortium treatment. Biotechnol Biofuels Bioprod 16:1–15. https://doi.org/10.1186/s13068-023-02306-2
26. Navarro A, Montiel C, Gracia-Fadrique J et al (2023) Supercritical carbon dioxide "explosion" on blue agave bagasse to enhance enzymatic digestibility. Biomass Convers Biorefinery 13:5691–5699. https://doi.org/10.1007/s13399-021-01557-z
27. Garuti M, Sinisgalli E, Soldano M et al (2022) Mechanical pretreatments of different agri-based feedstock in full-scale biogas plants under real operational conditions. Biomass Bioenergy 158:. https://doi.org/10.1016/j.biombioe.2022.106352
28. Al Afif R, Pfeifer C (2021) Enhancement of methane yield from cotton stalks by mechanical pre-treatment. Carbon Resour Convers 4:164–168. https://doi.org/10.1016/j.crcon.2021.04.003
29. Bai X, Wang G, Zhu Z et al (2020) Investigation of improving the yields and qualities of pyrolysis products with combination rod-milled and torrefaction pretreatment. Renew Energy 151:446–453. https://doi.org/10.1016/j.renene.2019.11.040
30. Sitotaw YW, Habtu NG, Gebreyohannes AY et al (2021) Ball milling as an important pretreatment technique in lignocellulose biorefineries: a review. Biomass Convers Biorefinery. https://doi.org/10.1007/s13399-021-01800-7
31. ASABE (2012) Method of determining and expressing particle size of chopped forage materials by Screening:3
32. Nava JV, Llorens T, Menéndez-Aguado JM (2020) Kinetics of dry-batch grinding in a laboratory-scale ball mill of Sn–Ta–Nb minerals from the Penouta Mine (Spain). Metals (Basel) 10:1–19. https://doi.org/10.3390/met10121687
33. Hamze H, Akia M, Yazdani F (2015) Optimization of biodiesel production from the waste cooking oil using response surface methodology. Process Saf Environ Prot 94:1–10. https://doi.org/10.1016/j.psep.2014.12.005
34. Ayodele BV, Cheng CK (2015) Modelling and optimization of syngas production from methane dry reforming over ceria-supported cobalt catalyst using artificial neural networks and Box-Behnken design. J Ind Eng Chem 32:246–258. https://doi.org/10.1016/j.jiec.2015.08.021
35. Senthilkumar T, Selvakumar A, Senthilkumar B (2023) Fabrication and optimization of activated carbon using sisal fiber biomass through Box-Behnken experimental design. Biomass Convers Biorefinery. https://doi.org/10.1007/s13399-023-04185-x
36. Farizhandi AAK, Zhao H, Chen T, Lau R (2020) Evaluation of material properties using planetary ball milling for modeling the change of particle size distribution in a gas-solid fluidized bed using a hybrid artificial neural network-genetic algorithm approach. Chem Eng Sci 215:115469. https://doi.org/10.1016/j.ces.2020.115469
37. Taşdemir A, Taşdemir T (2009) A comparative study on PSD models for chromite ores comminuted by different devices. Part Part Syst Charact 26:69–79. https://doi.org/10.1002/ppsc.200800035
38. Knieke C, Sommer M, Peukert W (2009) Identifying the apparent and true grinding limit. Powder Technol 195:25–30. https://doi.org/10.1016/j.powtec.2009.05.007
39. Ardit M, Molinari C, Verucchi D et al (2023) Microstructure and phase evolution of micronized ceramic colorants from a pilot plant for inks production. Ceram Int 49:882–893. https://doi.org/10.1016/j.ceramint.2022.09.061
40. Liu X-L, Fang Z, Tian X-F, Miao Z-D (2023) Effect of alkali salt-coupled ball milling pretreatment of wheat straw on improving enzymatic hydrolysis and energy efficiency. Fuel 340:127336. https://doi.org/10.1016/j.fuel.2022.127336
41. Gu BJ, Wang J, Wolcott MP, Ganjyal GM (2018) Increased sugar yield from pre-milled Douglas-fir forest residuals with lower energy consumption by using planetary ball milling. Bioresour Technol 251:93–98. https://doi.org/10.1016/j.biortech.2017.11.103
42. Erdemir F (2017) Study on particle size and X-ray peak area ratios in high energy ball milling and optimization of the milling parameters using response surface method. Meas J Int Meas Confed 112:53–60. https://doi.org/10.1016/j.measurement.2017.08.021
43. Roa DF, Santagapita PR, Buera MP, Tolaba MP (2014) Ball milling of amaranth starch-enriched fraction. Changes on particle size, starch crystallinity, and functionality as a function of milling energy. Food Bioprocess Technol 7:2723–2731. https://doi.org/10.1007/s11947-014-1283-0
44. Loubes MA, González LC, Tolaba MP (2022) Modeling energy requirements in planetary ball milling of rice grain. Part Sci Technol 40:66–73. https://doi.org/10.1080/02726351.2021.1906368
45. Kratky L, Jirout T (2022) Experimental identification and modelling of specific energy requirement for knife milled beech chips in dependence on particle size characteristics and moisture. Energy 243:122749. https://doi.org/10.1016/j.energy.2021.122749
46. Politiek RGA, Bruins ME, Keppler JK, Schutyser MAI (2022) Effect of oil content on pin-milling of soybean. J Food Eng 334:111149. https://doi.org/10.1016/j.jfoodeng.2022.111149
47. Menéndez M, Muñiz Sierra H, Gent M, de Cos Juez FJ (2018) The comminution energy-size reduction of the Bond Mill and its relation to Vickers hardness. Miner Eng 119:228–235. https://doi.org/10.1016/j.mineng.2018.01.017
48. Kratky L, Jirout T (2011) Biomass size reduction machines for enhancing biogas production. Chem Eng Technol 34:391–399. https://doi.org/10.1002/ceat.201000357